DOI: 10.61782/fa.2023.0630

forum acusticum 2023

COMPUTATIONAL CHARACTERIZATION OF FUNCTIONALLY GRADED POROUS ABSORBERS BASED ON TRIPLY PERIODIC MINIMAL SURFACES (TPMS)

Xueying Guan[1*] **Jieun Yang**[1] **Elke Deckers**[2,3]
Maarten Hornikx[1]

[1] Department of the Built Environment, Eindhoven University of Technology, The Netherlands
[2] Department of Mechanical Engineering, KU Leuven, Belgium
[3] Flanders Make@KU Leuven, Diepenbeek, Belgium

ABSTRACT

Triply periodic minimal surfaces (TPMS), a class of periodic implicit surface with zero mean curvature, are emerging as an excellent solution to create graded porous structures. The grading of a porous layer can enhance and broaden the acoustic absorption in a target frequency range. The porosity gradient within the TPMS structure can be precisely controlled by a mathematical function, straightforwardly allowing for optimization towards the desired absorption. As the first step of the optimization procedure, we present a computational approach to determine acoustic absorption properties of functionally graded TPMS porous structures: the transport parameters of a rigid-frame homogeneous TPMS porous absorber are found by the finite element simulations of three static problems, then the absorption coefficient of the TPMS porous structure with graded porosity along the thickness is calculated with the transfer matrix method. The presented approach is validated by direct numerical simulations of the same porous structure.

Keywords: *Periodic porous material, porosity grading, sound absorption, TPMS, homogenization, TMM*

Corresponding author: *x.guan1@tue.nl.*

1. INTRODUCTION

Porous materials consist of solid and fluid phases [1], and absorb sound energy mainly through viscous and thermal dissipation due to the fluid-solid interaction [2]. Hence, the sound absorption properties of a porous material largely depend on its microstructure [3]. The highly random microstuctures of traditional porous foams leads to difficulties in controlling and predicting their sound absorption performance [1]. In recent years, novel periodic porous materials formed by a repetition of a unit cell have been produced with additive manufacturing techniques, allowing the sound absorption spectrum to be customized for different applications [4].

The porous material can be macroscopically characterized by an effective density $\rho_e(\omega)$ accounting for inertial and viscous effects, and an effective bulk modulus $K_e(\omega)$ accounting for thermal effects [5]. For a periodic porous material, these macroscopic properties can be derived from boundary value problems (BVPs) at the microscale over a representative elementary volume (REV) (in this case the periodic unit cell) with the multiscale homogenization method [6]. A number of recent studies on periodic porous materials [4, 6, 7] numerically calculate transport parameters from the REV with finite element (FE) simulations. These transport parameters are then used as inputs for semi-phenomenological models such as the Johnson-Champoux-Allard-Lafarge (JCAL) model to obtain the effective density $\rho_e(\omega)$ and effective bulk modulus $K_e(\omega)$.

Efforts have also been made to enhance and broaden the sound absorption spectrum of periodic porous materi-

als through graded or multilayer structures [8–10], which have space-dependent effective properties optimized for acoustic absorption. Different numerical techniques, for example, the transfer matrix method (TMM) [10], Peano series [9], and transfer Green's functions [8], have been utilized to calculate the absorption coefficient of such graded or multilayer porous material.

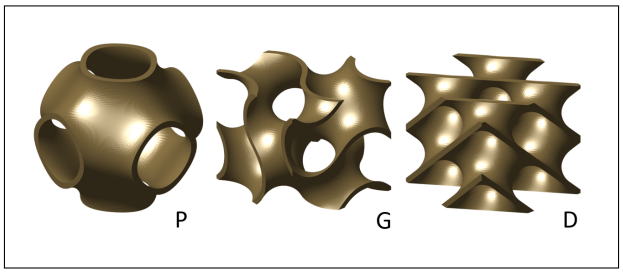

Figure 1: Common types of TPMS cells: Primitive (P), Gyroid (G) and Diamond (D).

Compared to other kinds of geometries used for periodic porous materials, triply periodic minimal surfaces (TPMS) (Fig. 1) have some unique attributes: they are generated by mathematical functions with parameters to precisely control the porosities or periodicity in every position within the structures; unlike the sharp edges of strut-based lattice structures, they have smooth surfaces that reduce the stress concentrations and enhance the mechanical properties; their pores are interconnected and have high surface-area-to-volume ratios [11]. These features make TPMS particularly suitable for multifunctional applications.

However, studies on acoustic properties of TPMS structures are rather limited and their full potential as sound absorbers still remains to be explored. The previous research on TPMS sound absorbers only focused on impedance tube measurements of 3D printed samples [12], but they have not yet been acoustically characterized from the unit cell geometry with a bottom-up approach. Furthermore, graded TPMS structures have not been previously used or optimized for acoustic applications. As the first step in the optimization procedure, the graded TPMS porous structures are acoustically characterized with homogenization techniques and the TMM in this paper. This approach is validated by direct numerical simulations (DNS).

The paper is organized as follows. The characterization method of graded TPMS structures and the numerical validation procedure is presented in Section 2. The results are discussed in Section 3. Section 4 summarizes the main findings and makes suggestions towards future work.

2. METHODS

This section briefly explains the procedures to characterize and validate acoustic properties of a graded TPMS absorber.

2.1 TPMS geometry generation

In this study, we use the primitive (P) type TPMS cell, an isotropic unit cell with cubic symmetry. The mathematical function to generate the primitive TPMS surface $\varphi_P(x, y, z)$ is as follows [13]:

$$\varphi_P(x, y, z) = \cos(\frac{2\pi}{T}x) + \cos(\frac{2\pi}{T}y) + \cos(\frac{2\pi}{T}z) = t, \quad (1)$$

where T is the period in x, y, z directions and is equal to the unit cell size l. t is the iso-value of the equation.

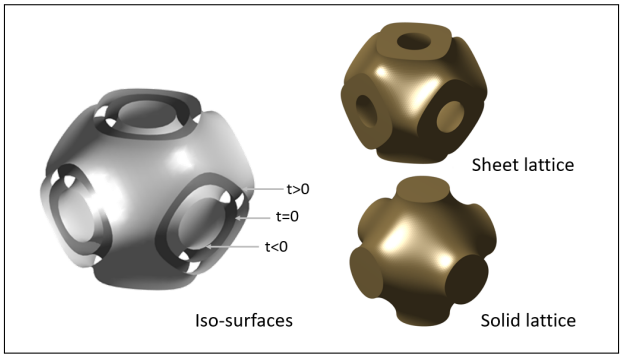

Figure 2: The TPMS geometry generation.

When the iso-value $t = 0$, the formula creates an iso-surface that divides the whole space into two equal volumes (Fig. 2). When $t \neq 0$, the generated iso-surface is offset from the zero-iso-value surface (Fig. 2). By setting an inequality $-t \leq \varphi(x, y, z) \leq t$ (assuming $t > 0$), the domain between surfaces with iso-value t and $-t$ is defined as solid, which is called a sheet lattice (Fig. 2) [14]. If the inequality $\varphi(x, y, z) \geq t$ or $\varphi(x, y, z) \leq -t$ is taken, then a so-called solid lattice can be generated (Fig. 2) [14]. For sheet lattices, t is directly related to the thickness of the wall, thereby controlling the porosity. Eqn. (2) gives the relationship between the iso-value t of a primitive TPMS sheet lattice and the porosity ϕ:

$$t = -1.7390\phi + 1.7426 \quad (2)$$

The porosity grading of the TPMS can be achieved by setting t as a continuous function of the position (x, y, z) [13]. Geometry models of sheet TPMS lattices with single porosities or functional gradings are generated with MSLattice, developed by Al-Ketan and Abu Al-Rub [14], then imported into COMSOL Multiphysics for FE simulations.

2.2 Homogenization approach to characterize TPMS lattices with a single porosity

To obtain the effective properties of single-porosity TPMS lattices, a hybrid multiscale homogenization approach with the JCAL model [6] is utilized. The six JCAL parameters are derived from TPMS geometries and FE simulations of three static BVPs in the fluid domain of a TPMS unit cell: the Stokes' flow problem, the electric conduction problem, and the Poisson's problem. The implementation details can be found in a paper by Zieliński et al. [6]. These parameters are the porosity ϕ, the high frequency limit of tortuosity a_∞, the static viscous permeability k_0, the static thermal permeability k_0', the viscous characteristic length Λ and thermal characteristic length Λ'. These numerically computed parameters are then used to calculate the frequency-dependent viscous and thermal dynamic tortuosities $a(\omega)$ and $a'(\omega)$ with the JCAL model. The details of the JCAL model can be also found in [6]. Tab. 1 gives the fluid properties used in the calculation.

Table 1: The fluid properties.

Fluid properties	Value
Density ρ_0	$1.2\ \mathrm{kg/m^3}$
Dynamic viscosity η	$1.82\ \times 10^{-5}\mathrm{N\cdot s/m^2}$
Thermal conductivity λ	$2.6 \times 10^{-2}\ \mathrm{W/(m\cdot K)}$
Specific heat capacity c_p	$1006\ \mathrm{J/(kg\cdot K)}$
Atmospheric pressure P_0	$101320\ \mathrm{Pa}$
Specific heat ratio γ	1.4
Speed of sound c_0	$343\ \mathrm{m/s}$

Once $a(\omega)$ and $a'(\omega)$ are known, the effective density $\rho_e(\omega)$ and bulk modulus $K_e(\omega)$ can be calculated from the following expressions:

$$\rho_e(\omega) = \frac{\rho_0 a(\omega)}{\phi}, \tag{3}$$

$$K_e(\omega) = \frac{\gamma P_0}{\phi}\left(\gamma - \frac{(\gamma-1)}{a'(\omega)}\right)^{-1}. \tag{4}$$

Then the wave number k and the characteristic impedance Z_c of the porous material can be determined by

$$k = \omega\sqrt{\frac{\rho_e(\omega)}{K_e(\omega)}}, \tag{5}$$

$$Z_c = \sqrt{\rho_e(\omega)K_e(\omega)}. \tag{6}$$

The surface impedance Z_s of a single layer of rigidly-backed porous material with a thickness d is calculated by

$$Z_s = -\mathrm{j}Z_c cot(kd). \tag{7}$$

From the surface impedance we can further determine the normal incidence reflection coefficient R and the absorption coefficient α of the rigidly-backed porous layer:

$$R = \frac{Z_s - \rho_0 c_0}{Z_s + \rho_0 c_0}, \tag{8}$$

$$\alpha = 1 - |R|^2. \tag{9}$$

2.3 Transfer matrix method to characterize graded TPMS structures

The TMM [5] is used to predict the acoustic properties of the graded TPMS. In this method, the continuously-graded TPMS is regarded as a multilayer structure with layers of constant properties (Fig. 3), and each layer i is represented by a 2 × 2 matrix $\mathbf{TM}^{(i)}$ expressed in terms of the thickness of the layer, t_i, its wave number, k_i, and its characteristic impedance, Z_i:

$$\mathbf{TM}^{(i)} = \begin{bmatrix} \cos(k_i t_i) & \mathrm{j}Z_i \sin(k_i t_i) \\ \frac{\mathrm{j}\sin(k_i t_i)}{Z_i} & \cos(k_i t_i) \end{bmatrix}. \tag{10}$$

The total transfer matrix $\mathbf{TM}$ of the graded TPMS are then calculated by multiplying the transfer matrix of each layer:

$$\mathbf{TM} = \prod_{i=1}^{N} \mathbf{TM}^{(i)}. \tag{11}$$

The surface impedance Z_s of a rigidly-backed graded TPMS absorber can be obtained with Eqn. (12) [10]:

$$Z_s = \frac{\mathrm{TM}_{11}}{\mathrm{TM}_{21}}, \tag{12}$$

where the subscripts of TM denote the matrix components. Similar to the single-porosity case, Eqn. (8) and Eqn. (9) are used to calculate the normal incidence absorption coefficient of graded TPMS structures.

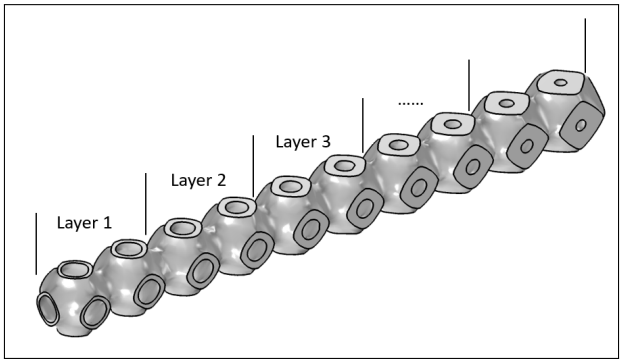

Figure 3: The continuously-graded TPMS is regarded as a multilayer absorber in TMM.

2.4 Validation by direct numerical simulations

Alternatively, the sound field in the porous microstructure can be computed with the DNS to obtain the absorption coefficient [6]. The Navier-Stokes-Fourier equation is solved in the fluid domain inside a band of TPMS porous material using the thermoviscous acoustics module in COMSOL Multiphysics 6.0. No slip and isothermal conditions are applied to the fluid-solid interface and the hard backing. An adjacent thin layer of air is coupled to the porous layer to apply a plane wave excitation. The pressure acoustic module in COMSOL is used to solve the Helmholtz equation in this air layer. To reduce the computational cost, only 1/4 of the symmetric TPMS geometry is used in the simulation and symmetry conditions are applied to the lateral boundaries. The DNS is performed for the frequency range between 500 Hz and 10000 Hz, with a 500 Hz step. The absorption coefficient is calculated from the reflection coefficient, determined by dividing the reflected pressure by the incident pressure at a point in the thin air layer. Fig. 4 illustrates the geometry in the DNS. The average relative difference ϵ between the absorption coefficients obtained from the homogenization method with the JCAL model and the DNS is calculated with Eqn. (13):

$$\epsilon = \frac{1}{n}\sum_{i=1}^{n}\frac{|a_{DNS}(f_i) - a_{JCAL}(f_i)|}{a_{DNS}(f_i)}, \qquad (13)$$

where n means the number of frequencies used in the DNS.

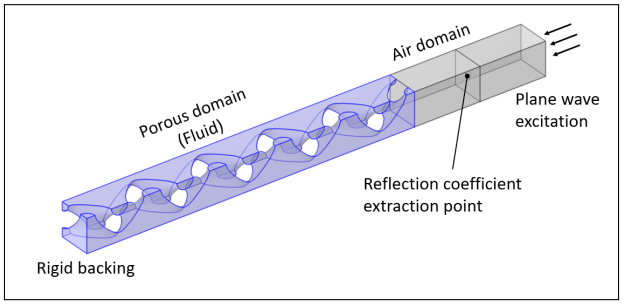

Figure 4: The geometry in the direct numerical simulation.

3. RESULTS AND DISCUSSION

In this section, we present the computational results obtained from the characterization and validation procedures.

3.1 Simulated JCAL parameters

JCAL parameters of TPMS primitive cells with three different unit cell sizes (l = 0.5 mm, 1 mm, 2 mm) and 9 different porosities ϕ (50%-90%, every 5%) are calculated from FE simulations on a REV. The relationship between JCAL parameters (k_0, k_0', Λ, Λ' and a_∞) and geometrical parameters (porosity ϕ and unit cell size l) of TPMS unit cells are shown in Fig. 5. The simulated JCAL parameters monotonically increase with the porosity and the unit cell size of the TPMS structure, except for the high frequency limit of tortuosity a_∞, which does not depend on the unit cell size and decreases with the porosity.

In order to discover the relationship between the JCAL parameters and the unit cell size, the permeabilities k_0 and k_0' (with unit m^2) are normalized by the square of the unit cell size l^2, while the characteristic lengths Λ and Λ' (with unit mm) are normalized by the unit cell size l. Fig. 6 shows the relationship between the geometrical parameters and normalized JCAL parameters. It is found that the normalized JCAL parameters do not depend on the size of the unit cell, which makes it possible to obtain the JCAL parameters of TPMS cells of any size by only performing simulations with cells of one size.

3.2 Validation of hybrid homogenization results against DNS: single-porosity TPMS absorbers

The homogenization method used in this study is valid when the condition of separation of scales is fulfilled,

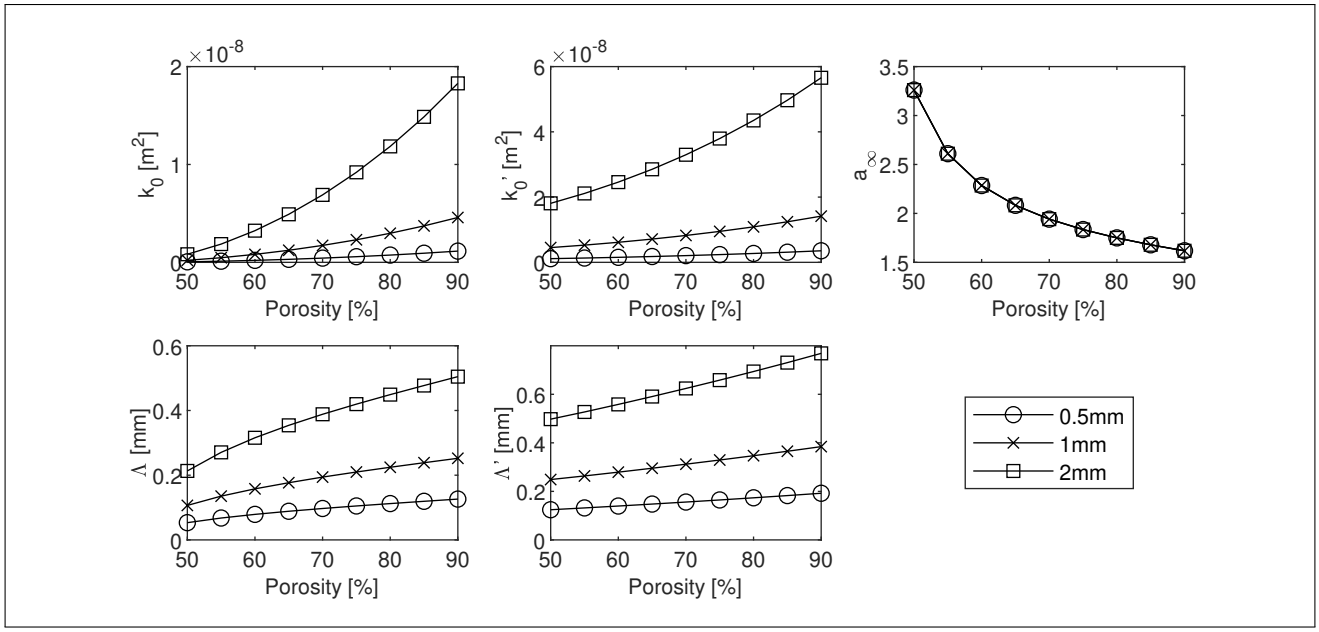

Figure 5: Simulated JCAL parameters considering three unit cell sizes and different porosities

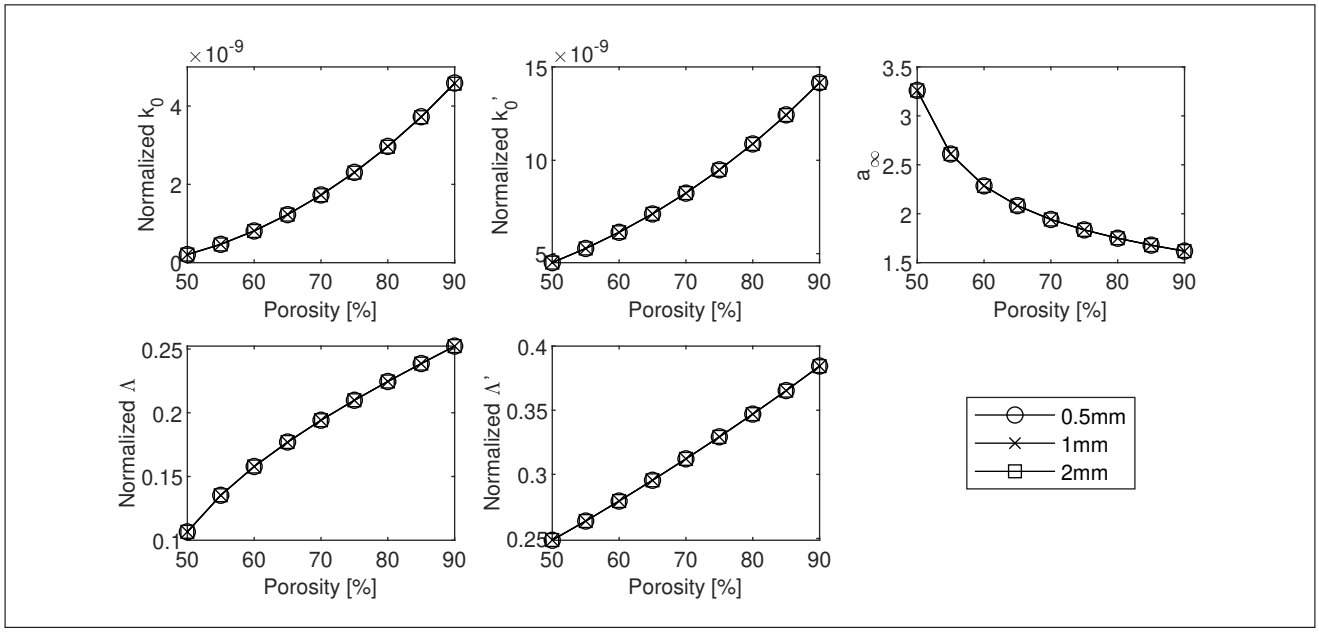

Figure 6: Normalized JCAL parameters considering three unit cell sizes and different porosities

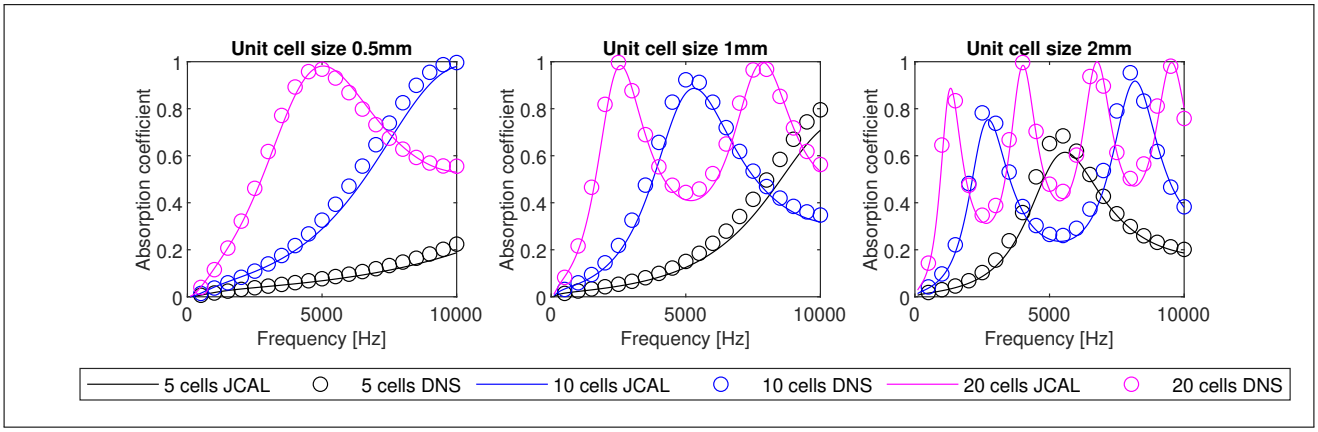

Figure 7: DNS validation: single porosity TPMS absorber

meaning the size of the unit cell should be sufficiently small compared to the macroscopic dimensions of the porous layer and the wavelength [15]. We verify this condition by the DNS of single-porosity TPMS absorbers (ϕ = 60%) with different cell sizes (0.5 mm, 1 mm, 2 mm) and different number of cells (5, 10, 20) along the thickness. Sufficiently fine meshes are used in the simulations to ensure the convergence of results. In Fig. 7, the results of hybrid homogenization with the JCAL model are presented alongside the DNS results. The relative difference ϵ between the homogenization and the DNS results can be found in Tab. 2. Generally, the difference ϵ between the homogenization and the DNS results decreases with increasing number of cells along the thickness. The difference is within 10% when using more than 10 cells. Compared to the number of cells, the cell size does not significantly influence the homogenization results, likely because it is much smaller than the wavelength. However, when the porous layer is sufficiently thick, for instance the 20 cells case, a larger unit cell leads to a slightly greater difference from the DNS result.

Table 2: The difference ϵ: single-porosity absorbers

Cell size	5 cells	10 cells	20 cells
0.5 mm	11.17%	7.92%	3.49%
1 mm	14.54%	7.90%	4.83%
2 mm	10.37%	8.70%	6.04%

3.3 Validation of homogenization + TMM results against DNS: graded TPMS absorber

We calculate the absorption coefficients of 10mm-thick graded TPMS absorbers with two kinds of porosity profiles (Fig. 8): a linear profile and a S-curve profile created by the logistic function. We choose these profiles in order to investigate how well the characterization approach in this study can predict the absorption coefficient of a graded TPMS absorber with a steep porosity gradient. Both have a unit cell size of 1 mm, 50% porosity on the rigid backing (d = 0 mm) and higher porosity towards the top surface (d = 10 mm). One has a gradual porosity transition while the other has a more abrupt porosity change around d = 5 mm. The graded TPMS geometry used in DNS can be seen in Fig. 9. The reverses of these profiles are also studied, which have a decreasing porosity along the thickness.

The comparison of the homogenization + TMM results and DNS results is presented in Fig. 10. The layer resolution t_i of the TMM is 1 mm. A good agreement between the both results is found, hence the homogenization + TMM approach can accurately characterize a graded TPMS absorber with a relatively steep porosity gradient. Tab. 3 shows the relative difference ϵ between these results using different TMM layer resolutions t_i. For the TPMS absobers with an increasing porosity along the thickness (Linear and S-curve), the homogenization + TMM approach deviates more from the DNS results, compared to the absorbers with a decreasing porosity (L-reverse and S-reverse). The layer resolution t_i in TMM also slightly influences the results. It is found that a layer resolution of

2 mm leads to the smallest error.

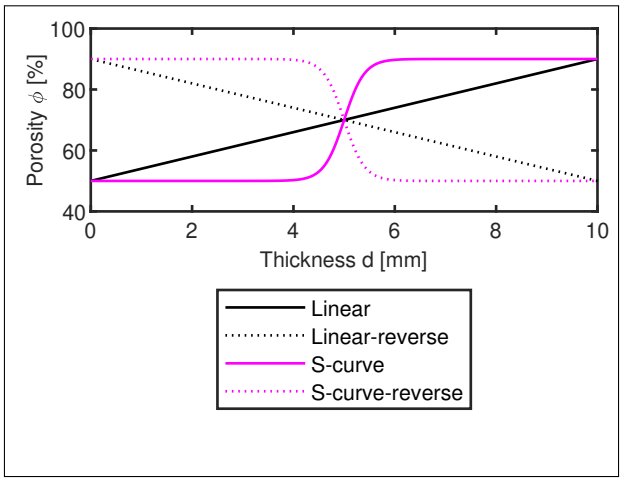

Figure 8: Porosity profile of the graded TPMS absorbers

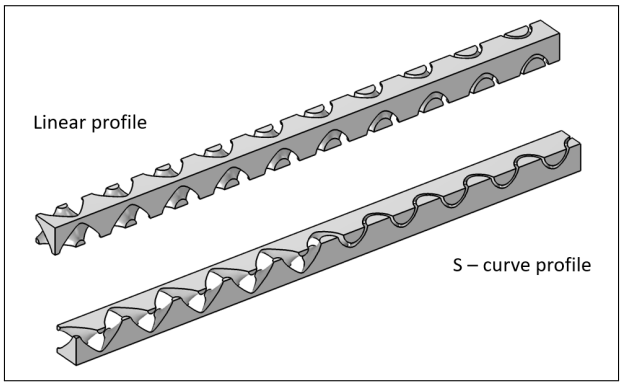

Figure 9: Geometry of the graded TPMS absorbers in DNS

Table 3: The difference ϵ: graded absorbers.

Profile	t_i= 0.5 mm	t_i= 1 mm	t_i= 2 mm
Linear	10.06%	10.02%	9.88%
S-curve	8.43%	8.76%	4.63%
L-reverse	5.76%	5.34%	3.98%
S-reverse	5.48%	5.70%	3.74%

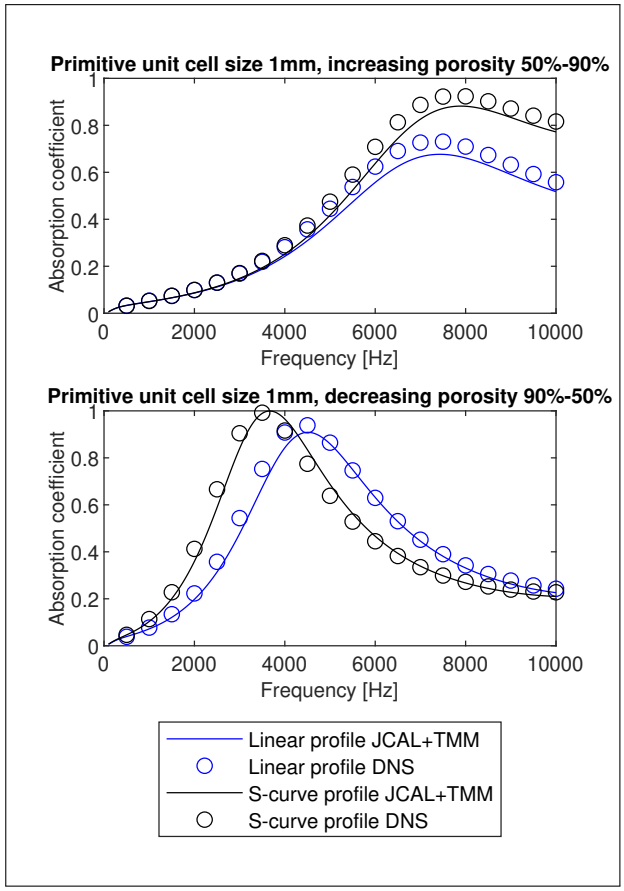

Figure 10: DNS validation: graded TPMS absorber, unit cell size 1mm, porosity range 50%-90%.

4. CONCLUSIONS

In this study, we computationally characterized the primitive type TPMS porous absorber by the hybrid homogenization with the JCAL model. The JCAL parameters of primitive TPMS cells with various porosities and sizes are obtained by the FE simulations of three static BVPs performed within the REV. Useful relations are found between the geometrical parameters and the JCAL parameters, which can simplify the design of TPMS absorbers. The validation of the hybrid homogenization results against the DNS are also presented. The homogenization results of single-porosity TPMS absorbers agree well with the DNS when a good separation of scale is ensured: the error lies within 10% if the number of cells along the porous layer thickness exceeds 10. Graded TPMS absorbers with a relatively steep porosity gradient

are shown to be accurately characterized with the homogenization + TMM approach, with an error within or slightly above 10%. The future steps will be the optimization of functionally-graded TPMS acoustic absorbers and the experimental validation of the numerical results.

5. REFERENCES

[1] O. Doutres, M. Ouisse, N. Atalla, and M. Ichchou, "Impact of the irregular microgeometry of polyurethane foam on the macroscopic acoustic behavior predicted by a unit-cell model," *The Journal of the Acoustical Society of America*, vol. 136, no. 4, pp. 1666–1681, 2014.

[2] T. J. Cox and P. D'Antonio, *Acoustic absorbers and diffusers: theory, design and application*. London ; New York: Taylor & Francis, 3rd ed ed., 2017.

[3] K. Gao, J. A. W. van Dommelen, and M. G. D. Geers, "Investigation of the effects of the microstructure on the sound absorption performance of polymer foams using a computational homogenization approach," *European Journal of Mechanics - A/Solids*, vol. 61, pp. 330–344, 2017.

[4] S. Deshmukh, H. Ronge, and S. Ramamoorthy, "Design of periodic foam structures for acoustic applications: Concept, parametric study and experimental validation," *Materials & Design*, vol. 175, p. 107830, 2019.

[5] J. Allard and N. Atalla, *Propagation of Sound in Porous Media: Modelling Sound Absorbing Materials, Second Edition*. Wiley, 2009.

[6] T. G. Zieliński, R. Venegas, C. Perrot, M. Červenka, F. Chevillotte, and K. Attenborough, "Benchmarks for microstructure-based modelling of sound absorbing rigid-frame porous media," *Journal of Sound and Vibration*, vol. 483, p. 115441, 2020.

[7] J. Boulvert, J. Costa-Baptista, T. Cavalieri, M. Perna, E. R. Fotsing, V. Romero-García, G. Gabard, A. Ross, J. Mardjono, and J.-P. Groby, "Acoustic modeling of micro-lattices obtained by additive manufacturing," *Applied Acoustics*, vol. 164, p. 107244, 2020.

[8] J. Boulvert, T. Cavalieri, J. Costa-Baptista, L. Schwan, V. Romero-García, G. Gabard, E. R. Fotsing, A. Ross, J. Mardjono, and J.-P. Groby, "Optimally graded porous material for broadband perfect absorption of sound," *Journal of Applied Physics*, vol. 126, no. 17, p. 175101, 2019.

[9] T. Cavalieri, J. Boulvert, L. Schwan, G. Gabard, V. Romero-Garcìa, J.-P. Groby, M. Escouflaire, and J. Mardjono, "Acoustic wave propagation in effective graded fully anisotropic fluid layers," *The Journal of the Acoustical Society of America*, vol. 146, no. 5, pp. 3400–3408, 2019.

[10] J. Costa-Baptista, E. R. Fotsing, J. Mardjono, D. Therriault, and A. Ross, "Design and fused filament fabrication of multilayered microchannels for subwavelength and broadband sound absorption," *Additive Manufacturing*, vol. 55, p. 102777, 2022.

[11] J. Feng, J. Fu, X. Yao, and Y. He, "Triply periodic minimal surface (TPMS) porous structures: from multi-scale design, precise additive manufacturing to multidisciplinary applications," *International Journal of Extreme Manufacturing*, vol. 4, no. 2, p. 022001, 2022.

[12] W. Yang, J. An, C. K. Chua, and K. Zhou, "Acoustic absorptions of multifunctional polymeric cellular structures based on triply periodic minimal surfaces fabricated by stereolithography," *Virtual and Physical Prototyping*, vol. 15, no. 2, pp. 242–249, 2020.

[13] F. Liu, Z. Mao, P. Zhang, D. Z. Zhang, J. Jiang, and Z. Ma, "Functionally graded porous scaffolds in multiple patterns: New design method, physical and mechanical properties," *Materials & Design*, vol. 160, pp. 849–860, 2018.

[14] O. Al-Ketan and R. K. Abu Al-Rub, "MSLattice: A free software for generating uniform and graded lattices based on triply periodic minimal surfaces," *Material Design & Processing Communications*, vol. 3, no. 6, p. e205, 2021.

[15] J.-L. Auriault, "Homogenization theory applied to porous media," *Poromechanics III: Biot Centennial (1905-2005) - Proc. of the 3rd Biot Conference on Poromechanics*, pp. 113–120, 2005.